# Incorporation of nitrogen in Co:ZnO studied by x-ray absorption spectroscopy and x-ray linear dichroism

D. Schauries,[1,*] V. Ney,[1,2] S. K. Nayak,[1] P. Entel,[1] A. A. Guda,[3] A. V. Soldatov,[3] F. Wilhelm,[4] A. Rogalev,[4] K. Kummer,[4] F. Yakhou,[4] and A. Ney[1,2]

[1]*Fakultät für Physik, Universität Duisburg-Essen, Lotharstrasse 1, D-47057 Duisburg, Germany*

[2]*Institut für Halbleiter- und Festkörperphysik, Johannes Kepler Universität, Altenberger Strasse 69, 4040 Linz, Austria*

[3]*Research Center for Nanoscale Structure of Matter, Southern Federal University, Rostov-on-Don, Russia*

[4]*European Synchrotron Facility, 6 Rue Jules Horowitz, Boîte Postale 220, 38043 Grenoble Cedex, France*

(Received 11 December 2012; published 25 March 2013)

N-doped $Co_xZn_{1-x}O$ epitaxial films were grown by reactive magnetron sputtering using a range of different $N_2$ and $O_2$ concentrations. They were studied by x-ray absorption near edge spectroscopy (XANES) and x-ray linear dichroism (XLD). The incorporation of N into the ZnO host lattice could be determined via the XLD at the N $K$-edge in comparison with the O $K$-edge and respective simulations of XANES and XLD of the various dopant configurations. The addition of nitrogen predominantly leads to the formation of molecular nitrogen on O sites (split interstitial). Only for samples grown with very low $O_2$ partial pressure was a small fraction of the N found to substitute for O in its atomic form.

DOI: 10.1103/PhysRevB.87.125206 PACS number(s): 71.55.Gs, 78.70.Dm, 61.05.cj

## I. INTRODUCTION

During the last decade zinc oxide (ZnO) has been the subject of intense research. The availability of high-quality large ZnO single crystals, its wide (3.4 eV) and direct band gap, and its large exciton binding energy (60 meV) makes it an interesting substitution for GaN in optoelectronic applications.[1] With as-grown ZnO being $n$ type, most likely due to hydrogen impurities, $p$-doping remains a grand challenge for material science. Besides being a necessity for $pn$ junctions, $p$-type ZnO is of particular interest to investigate the perspectives for obtaining room-temperature ferromagnetism in transition metal [usually Mn-doped (Refs. 2 and 3) or Co-doped (Ref. 3)], $p$-type ZnO. As a shallow acceptor in other II–VI semiconductors atomic nitrogen is one of the most promising dopants for $p$ type.[1,4] Having electronegativity and size similar to those of oxygen, substitutional incorporation of atomic N on O lattice sites ($N_O$) is considered the most likely position for atomic N (Ref. 1). Early density functional theory (DFT) calculations have shown that in this position N indeed acts as a shallow acceptor in N-doped ZnO (ZnO:N) (Ref. 5). Others have come to the conclusion that $N_O$ is rather a deep acceptor[6,7] and therefore does not contribute to $p$-type behavior. However, a recent publication reports $N_O$ to be a shallow acceptor if additional codoping is employed.[8] Besides these contradictory theoretical results, DFT in general underestimates the band gap of ZnO significantly and related results have to be treated with caution.[9] Therefore, a direct experimental determination of the incorporation of N in ZnO and its location within the host lattice is very useful to complement the theoretical predictions.

Most studies on ZnO:N have focused on conductivity measurements, as summarized elsewhere,[10] but have not directly studied the position of N in ZnO. Also a light emitting diode (LED) based on $p$-type ZnO:N was reported to emit blue light;[11] however, considering ZnO to have a band gap of 3.4 eV one would rather expect emission of ultraviolet light. Thus, doubts on the reliability and reproducibility of the $p$-type doping arose.[1] A more direct experimental method to investigate the incorporation of N into ZnO is x-ray absorption near edge spectroscopy (XANES) because of its sensitivity to the local crystallographic structure and its element selectivity. XANES measurements at the N $K$-edge of ZnO:N samples have attributed certain peaks in the spectra to the formation of $N_O$ by comparison with simulations of XANES.[4,12] In contrast, other authors claim that most N-doping techniques predominantly lead to the incorporation of $N_2$ in its molecular form.[13,14] Thus, the different possible dopant species have to be identified in XANES by their respective spectroscopic signatures, similar to other N-containing compounds such as GaN (Ref. 15) and N-doped $SiO_2$ (Ref. 16). DFT calculations of the respective formation energies of ZnO:N show that molecular nitrogen incorporated on an O site [split interstitial, $(N_2)_O$] is the predominant species over a wide range of O concentrations, followed by interstitial molecules $(N_2)_i$ at very high oxygen partial pressures.[13] To the other end, for reduced oxygen partial pressures the formation energy of $N_O$ decreases and $[N_O\text{-}(N_2)_O]^+$ complexes become energetically favorable.[14]

Here we report on XANES measurements of N-doped $Co_xZn_{1-x}O$ (Co:ZnO:N) recorded with two orthogonal linear polarizations and the respective x-ray linear dichroism (XLD) to study the incorporation of N into the Co:ZnO host crystal in analogy to previous work where we have found that in comparable samples Co mainly substitutes for Zn (Refs. 17 and 18). It is shown that $(N_2)_{i/O}$ and $N_O$, although having similarities in their respective XANES spectra, exhibit different XLD signatures. Both XANES and XLD measurements and respective simulations of the N $K$-edges are compared with the O $K$-edge. It is revealed that mostly $(N_2)_O$ is formed for Co:ZnO:N. For reduced $O_2$ concentration a small fraction of N is found as $N_O$ as well. Both results corroborate recent DFT calculations.[13] Additional measurements at the Zn $K$-edge indicate that a reduced $O_2$ partial pressure during growth leads to the formation of O vacancies ($V_O$), which can be suppressed by increasing the $N_2$ partial pressure to promote the incorporation of nitrogen during growth.

 

## II. METHODS

Co:ZnO:N samples were grown on *c*-plane sapphire [$Al_2O_3(0001)$] at a temperature of 350°C by reactive magnetron sputtering from a metallic Zn/Co target. The base pressure of the ultrahigh vacuum sputtering system was $\leqslant 10^{-9}$ mbar. The working pressure in the chamber during film deposition was $4 \times 10^{-3}$ mbar. The sputter gas consisted of Ar as inert gas and a variable $O_2/N_2$ composition as reactive gas which was controlled via separated mass flow controllers. It has been shown before that samples grown with an Ar:$O_2$ ratio of 10:1 standard cubic centimeters per minute (sccm) exhibit the highest structural quality for Co concentrations from 5% to 15%.[18] For this work 10%, 15%, and 20% Co:ZnO samples with an $O_2$ flow from 1 down to 0.5 sccm and various Co:ZnO:N samples with reduced $O_2$ flow and $N_2$ concentrations from 0.3 to 1 sccm were grown. All sample series show comparable physical properties especially with regard to their structural properties as measured with x-ray diffraction and the XANES and XLD signatures. Since the 20% Co:ZnO sample series comprises the widest range of $O_2$:$N_2$ flow ratios this work focuses on the 20% Co:ZnO series as listed in Fig. 1. X-ray reflectivity measurements (XRR) showed thicknesses of $162 \pm 5$ nm for films with $N_2$ and $153 \pm 3$ nm for the Co:ZnO film grown with Ar:$O_2$ of 10:1 without $N_2$; the 10:0.5 sample was too rough to be measured with XRR.

The XANES measurements were carried out at the European Synchrotron Radiation Facility (ESRF). The XANES measurements of the N and O *K*-edges were recorded using soft x rays at ID08 and both total fluorescence yield (FY) and total electron yield (TEY); for the Zn *K*-edge hard x rays were used at ID12 in FY mode only. The information depth of the FY is in the range of 100 nm for soft x rays to 1 $\mu$m for hard x rays, while it is only a few nanometers for TEY, making this a surface-sensitive technique. All measurements were carried out at room temperature. Unless otherwise stated, all XANES spectra were normalized with respect to the edge jump. XLD was taken as the direct difference of two XANES

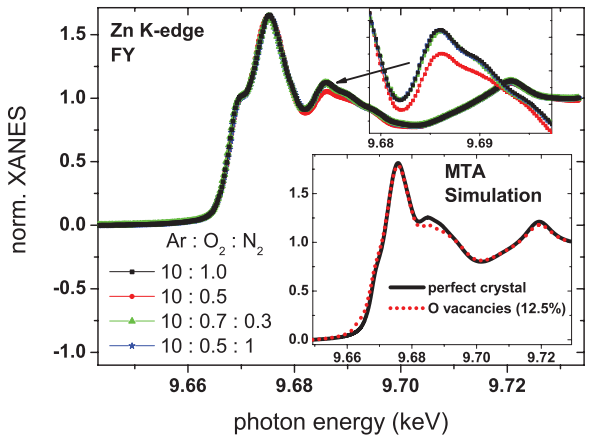


FIG. 1. (Color online) Zn *K*-edge of samples with four different sputter gas compositions. Only the film grown with Ar:$O_2$ = 10 : 0.5 shows a characteristic feature (arrow and top inset). The bottom inset shows respective MTA calculations with FDMNES for a defect-free crystal (line) and one with 12.5% $V_O$ (dots).

spectra recorded with vertical and horizontal polarized light under grazing incidences of 20° (ID08) and 10° (ID12), i. e., with the *E* vector of the light either parallel or perpendicular to the *c* axis of the Co:ZnO:N film. Details about ID08 and ID12 can be found elsewhere.[19,20]

The experimental spectra were complemented by respective simulations. As a first step to simulate the various XANES and XLD spectra the respective $2 \times 2 \times 2$ supercell of the Co:ZnO(:N) structure was relaxed. The generalized gradient approximation (GGA) using the Perdew-Burke-Ernzerhof exchange-correlation functional (PBE),[21] as implemented in the Vienna *ab initio* simulation package (VASP),[22] was employed for treating the interactions between the respective defect and the ZnO host lattice. The energy cutoff for the plane waves was set to 500 eV and the total energy tolerance for the relaxation was $10^{-8}$ eV. We have also checked the relaxations with the Perdew-Wang 91 functionals,[23] which are in agreement with those derived by the PBE functionals. In most cases the changes in the spectra due to the relaxation were found to be small, in particular for the Zn and O *K*-edges with and without O vacancies; the input structures for the N *K*-edge simulations are discussed in more detail in Sec. III. In general only the spectra derived from the relaxed structures are shown. The second step is to calculate the XANES and XLD spectra from the relaxed input structures. Three different methods were used. The FDMNES code[24] offers the option to use a multiple scattering formalism within the muffin-tin approximation (MTA) or a full-potential variant based on the finite difference method (FDM). Both methods are implemented in the same package and differ in the way the potential is derived. Wherever possible, the MTA was used because it is computationally much less demanding and time-consuming. In particular, the use of the MTA was possible for simulating atoms on lattice sites, such as the Zn *K*-edge and the O *K*-edge of ZnO and the N *K*-edge of $N_O$:ZnO. It was verified for the Zn and O *K*-edges of the undisturbed ZnO crystal that the FDM calculations yield results very similar to those of the MTA calculations, both of which agree well with the experimental data (not shown), so that the more tedious simulations were done using the MTA. For the N *K*-edge spectra of the $N_2$ molecule comparative simulations between the FDM and the MTA have shown that the FDM had to be used to yield spectra which are comparable with the experimental ones. We ascribe this to the fact that the strong covalent bonding and the small distance between the two N atoms in the molecule are not well accounted for by means of the MTA. In order to complement the FDMNES simulations, an independent full-potential linearized augmented plane-wave approximation (FPLAPW) was used as well which is implemented in the WIEN2K program package.[25]

## III. EXPERIMENTAL RESULTS AND MODELING

Figure 1 compares the normalized XANES at the Zn *K*-edge for four different Co:ZnO(:N) samples grown under various Ar:$O_2$(:$N_2$) sputter gas compositions. It can be clearly seen that all XANES spectra are virtually identical except for the film grown with Ar:$O_2$ of 10:0.5 which exhibits a clearly reduced absorption around 9.685 keV as marked by the arrow and enlarged in the top inset of Fig. 1. Both Co:ZnO:N films grown with a reduced $O_2$ partial pressure but

with the addition of $N_2$ ($Ar:O_2:N_2$ of 10:0.5:1 and 10:0.7:0.3, respectively) do not exhibit this reduction but coincide with the XANES of the reference 20% Co:ZnO sample grown without nitrogen ($Ar:O_2 = 10:1$). This sample yields the maximum possible size of the XLD signal of 1.1 (not shown) which indicates optimum structural quality.[18] Comparable results were obtained at the Co $K$-edges as well (not shown). To understand the origin of the reduced absorption for the 10:0.5 Co:ZnO sample, simulations were carried out for an ideal ZnO lattice as well as various defect configurations including $V_O$. For the simulations the wurtzite lattice parameters $a = 3.2459$ Å and $c = 5.2069$ Å as well as a dimensionless $u$ parameter of 0.382 for the vertical separation of the Zn and O atoms[26] were taken as successfully done before.[17] We also verified that the presence of the Co does not significantly alter the shape of the calculated Zn $K$-edge as long as the Co was substituting for Zn (not shown). A radius of 11 Å was chosen for the scattering sphere, corresponding to 468 atoms. Finally, the spectra were convoluted with a Lorentzian-like function to take the finite lifetimes of the excitations into account.[27] To simulate the $V_O$ one O atom was removed from the supercell and atomic positions were relaxed by minimizing the interatomic forces with the conjugate gradient algorithm. Subsequently all four adjacent Zn atoms were taken as the absorption center. Atoms further away from the $V_O$ did not show any deviation from the defect-free spectrum. The spectra of the four adjacent atoms were averaged. As this corresponds to a $V_O$ concentration of 25% the spectrum was averaged with the defect-free one to obtain an effective concentration of 12.5%. The result of the latter two simulations is shown in the lower inset of Fig. 1, where one observes that the reduction of the absorption found in the experiment at 9.685 keV is reproduced fairly well. Therefore the reduced $O_2$ partial pressure can be associated with the formation of $V_O$ which is in turn suppressed by the addition of $N_2$ to the sputter gas. This result already suggests that nitrogen is at least partially incorporated on O rather than on interstitial lattice sites.

Figure 2 shows the XANES using two orthogonal polarization directions $E \parallel c$ and $E \perp c$ (a) and the corresponding XLD (b) at the O $K$-edge of the 20% Co:ZnO grown with an $Ar:O_2$ ratio of 10:1 (solid symbols). The spectra were recorded in TEY and FY (not shown) and exhibit identical features of both XANES and XLD signals. The TEY spectra exhibit less self-absorption compared to the FY spectra and thus can be more easily and directly compared with the MTA (lines) and FPLAPW (open symbols) calculations which were carried out using the bulk ZnO lattice parameters as described above. Both simulations result in an overall good reproduction of the measurements which is slightly less for the FPLAPW, especially before the rising edge. Nonetheless, the overall good agreement of both types of simulations corroborate that the shape of the simulated spectra does not critically depend on the method used to derive the potential. However, it was found by systematic variation of the parameters used for the simulations that the fine structure at the rising edge and the associated oscillatory features in the XLD correlate with the radius of the scattering sphere used for the simulations. In addition, small changes in this region are visible if one includes the Co dopant atom in the supercell for the simulations, which however, did

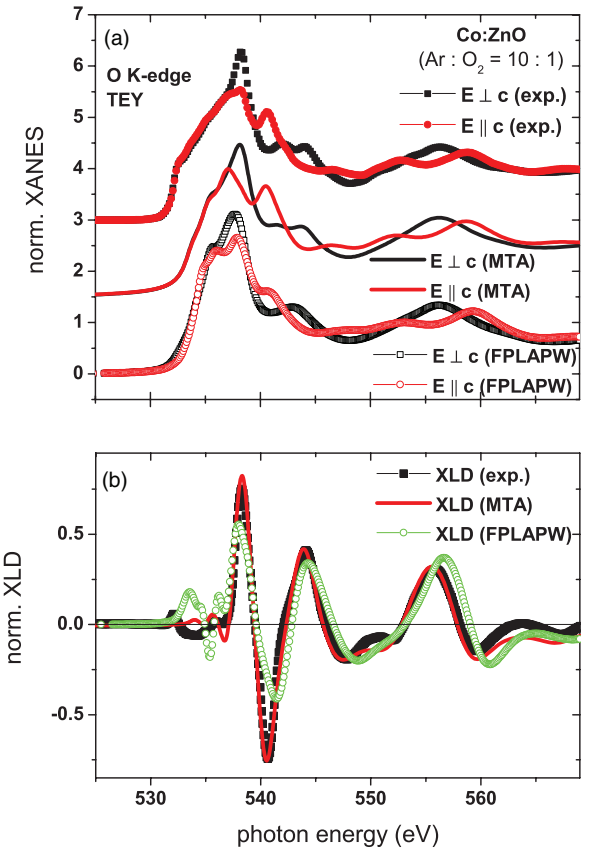


FIG. 2. (Color online) (a) Experimental (solid symbols) and calculated XANES at the O $K$-edge. Simulations were performed with MTA (lines) and FPLAPW (open symbols). (b) Respective measured and calculated XLD spectra.

not yield any systematic correlation (not shown), so that these features are considered not to be significant in the following. Therefore, the quantitative agreement of the XLD between experiment and simulations can be taken as an indication that the sample contains O predominantly in its atomic form on the proper anionic lattice site of the wurtzite ZnO.

Figure 3 shows experimental XANES (a) and respective XLD spectra (b) at the N $K$-edge in FY detection for an oxygen-rich Co:ZnO:N sample with $Ar:O_2:N_2 = 10:0.7:0.3$ in comparison to a pure Co:ZnO sample with $Ar:O_2 = 10:1$ (solid symbols). First, we discuss only the experimental spectra; the FDM simulations (lines) are discussed further below. The pure Co:ZnO sample shows neither a clear XANES signal nor a sizable XLD signal and consequently does not contain a sizable amount of nitrogen as expected. In contrast, the Co:ZnO:N sample exhibits clear XANES and XLD signals at the N $K$-edge measured in FY. This indicates that N is incorporated within the ZnO lattice, because FY spectra have an information depth of the order of the thickness of the samples. Because of the very low overall nitrogen content in these samples, self-absorption in the FY is less pronounced compared to the O $K$-edge. Note that the XANES recorded in the surface sensitive TEY mode (not shown) exhibits a very different XANES with a rather large background. Therefore the FY reflects the bulk properties of the samples; i.e., the nitrogen is incorporated within the bulk of the sample,

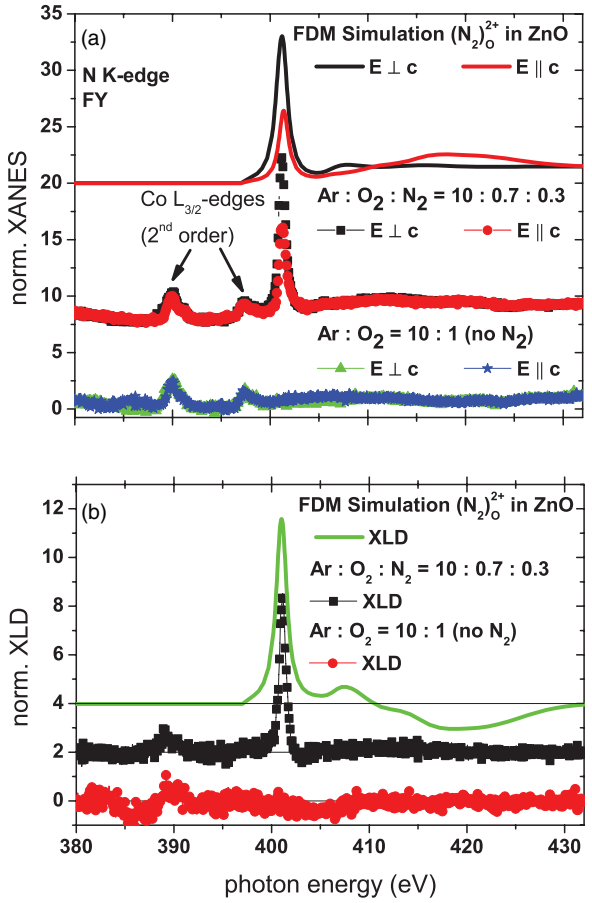


FIG. 3. (Color online) (a) Experimental XANES at the N $K$-edge for Co:ZnO:N with Ar:$O_2$:$N_2$ = 10 : 0.7 : 0.3 (squares and circles) and Co:ZnO with Ar:$O_2$ = 10 : 1 (triangles and stars), compared with a simulation of $N_2$ on an O-site split interstitial with an angle of 35° (lines). (b) Calculated (lines) and measured XLD for Co:ZnO:N (squares) and Co:ZnO (circles), respectively.

and the TEY data are disregarded in the following since they are presumably originating from nitrogen-containing contaminations of the surface which affect the TEY of N much more than the TEY of O, because O is present in much larger amounts in the sample. The two smaller peaks in both experimental spectra at ∼390 and ∼397 eV originate from the second-order light of the grating of the monochromator and they appear at half the energy of the Co $L_{3/2}$-edges (780 and 795 eV). Thus, they can be disregarded while discussing the properties of the N dopant atoms. Nonetheless, these peaks can serve to normalize the XANES since both samples contain a comparable amount of Co; a normalization with respect to the edge jump is prone to be erroneous because of the small overall amount of nitrogen and thus the very small edge jump. The most prominent peak in the N $K$-edge XANES at 401.1 eV only appears for the nitrogen-containing samples and its appearance and energy position are characteristic of the well-known $\pi^*$ resonance of the N-N bond of molecular nitrogen[28] suggesting that N is predominantly incorporated in its molecular form. It was even suggested that most of the molecular nitrogen in ZnO is incorporated in the form of gas bubbles.[4] However, the latter possibility is ruled out by the existence of a sizable XLD signal, since a gas would

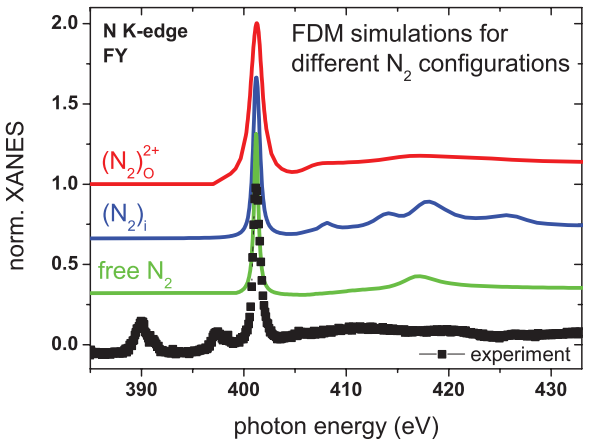


FIG. 4. (Color online) Experimental isotropic XANES at the N $K$-edge for the film grown with Ar:$O_2$:$N_2$ = 10 : 0.7 : 0.3. It is compared with FDM simulations for two different $N_2$ defects in ZnO and a free $N_2$ molecule. For the spectrum of the 35° orientated $(N_2)_O^{2+}$ defect anisotropic XANES and XLD are shown in Fig. 3.

imply random alignment of the molecules and thus lack any XLD signal. The clear dependence on the polarization and the associated XLD signal in Fig. 3(b) indicates a preferred orientation of the $N_2$ molecules which can be further analyzed. In general, the $\pi^*$ resonance shows the largest signal for x rays with perpendicular polarization with respect to the molecular axis. Since for all samples the absorption with polarization perpendicular to the $c$ axis is larger at 401.1 eV, the molecular axis has to be orientated with an average angle of less than 45° to the $c$ axis.

A more detailed analysis of the dominant N dopant species can be achieved by comparing the experimental XANES to different simulations to study the influence of the $N_2$ molecule's orientation and its surrounding crystal field on the XANES of the N $K$-edge via additional FDM simulations which are shown in Fig. 4. Various configurations for $N_2$ defects have been studied via DFT calculations predicting that $N_2$ molecules on $V_O$ should have a minimum energy for an angle of 35° with respect to the $c$ axis of ZnO (Ref. 14). Therefore, in Fig. 4 the experiment (black squares) is compared to a FDM simulation using the FDMNES code of a doubly charged nitrogen molecule $(N_2)^{2+}$ (to assure a bond length of 1.13 Å) located on an $V_O$ split interstitial, $(N_2)_O^{2+}$, with an angle of 35° with respect to the $c$ axis (top line in Fig. 4). The $\pi^*$ resonances of the experimental XANES and respective simulation are in good qualitative agreement as well as the size and shape in the energy range above 410 eV where the $\sigma^*$-shape resonance occurs. In addition, simulations of a neutral interstitial $N_2$ molecule, $(N_2)_i$ (middle line), parallel to the $c$ axis (bond length, 1.14 Å), and a free $N_2$ molecule (without the surrounding ZnO; lower line in Fig. 4) of comparable bond length (1.15 Å) are shown in Fig. 4. The resulting bond length correlates well with the charge state of the molecule and is known to shift the $\sigma^*$-shape resonance towards higher energies for shorter bond lengths.[29] All resulting spectra show the dominating $\pi^*$ resonance as observed in the experiment, which was used for normalization here. It can be noted that the influence of the surrounding crystal field on the $\pi^*$ resonance is weak and all simulated

spectra exhibit very similar $\sigma^*$-shape resonances which only differ by their respective fine structure while the $(N_2)_O^{2+}$ configuration has the least pronounced fine structure, which corresponds best to the experiment. Since this configuration is also energetically favored by DFT simulations,[14] for this configuration the polarization-dependent XANES and thus the resulting XLD were calculated using the FDM and the outcome is shown in Fig. 3 as lines. The comparison of the polarization-dependent experimental XANES and XLD at the N $K$-edge with the simulation of the $(N_2)_O^{2+}$ under 35°, which was predicted by DFT,[14] agrees rather well around the $\pi^*$ resonance whereas in the region of the $\sigma^*$-shape resonance the agreement is only satisfactory for the XANES while the simulated XLD shows a clear negative signal above ∼405 eV in contrast to the experiment, where essentially zero XLD is seen. However, a small distribution of the actual angle with respect to the $c$ axis, a fluctuation of the actual bond length associated with the charge state, may easily smear out the spectral details seen in the XLD simulations. Note in addition, that the experiment was carried out at 300 K while the simulations correspond to $T = 0$ K properties. Therefore, the comparison between the experiment and the simulations suggest that $(N_2)_O^{2+}$ under a finite angle of around 35° with respect to the $c$ axis with some distribution of charge state (and thus bond length) and orientation should be the dominant N dopant species in this sample. No signatures corresponding to atomic nitrogen are seen for this sample.

To promote the substitutional incorporation of N on O lattice sites ($N_O$), another Co:ZnO:N sample was grown under nitrogen-rich conditions ($Ar:O_2:N_2 = 10 : 0.5 : 1$). Figure 5 shows the measured XANES (a) and XLD (b) at the N $K$-edge (solid symbols) in comparison to simulated XANES and XLD $N_O$ spectrum using the MTA (lines) as well as FPLAPW (open symbols). First, it has to be noted that also in this sample the predominat spectral feature is the $\pi^*$ resonance as already observed for the oxygen-rich sample with less nitrogen in Fig. 3, which is cut off here to highlight the fine structure at higher photon energies. For the calculated spectra one N atom was placed on an O site and relaxed as for the Zn $K$-edge of ZnO with $V_O$. Both MTA and FPLAPW simulations reveal a spectral shape similar to that of the O $K$-edge of pure ZnO in Fig. 2. Comparable to the O $K$-edge, also at the N $K$-edge the MTA simulations have a slightly better agreement with the experimental data both for XANES and XLD if one disregards the predominant $\pi^*$ resonance in the experimental spectra. In addition, the simulations were fitted to the amplitudes of the experimental data, since only a small fraction of N is found to be incorporated on O sites with the majority of N remaining incorporated molecularly as indicated by a very pronounced $\pi^*$ resonance visible in Fig. 5(a). The XLD spectra show a good qualitative agreement between experiment and both simulations, whereas comparable signatures are not visible in the spectra of the Co:ZnO:N sample grown under oxygen-rich conditions ($Ar:O_2:N_2 = 10 : 0.7 : 0.3$). Additional measurements using the TEY on comparable samples, partially with reduced Co content (not shown), exhibit XLD signatures which are similar to the FY shown here. We therefore conclude that the increase of the $N_2$ and a simultaneous reduction of the $O_2$ partial pressure during preparation promotes the formation of $N_O$ which is in accordance with recent DFT simulations.[13]

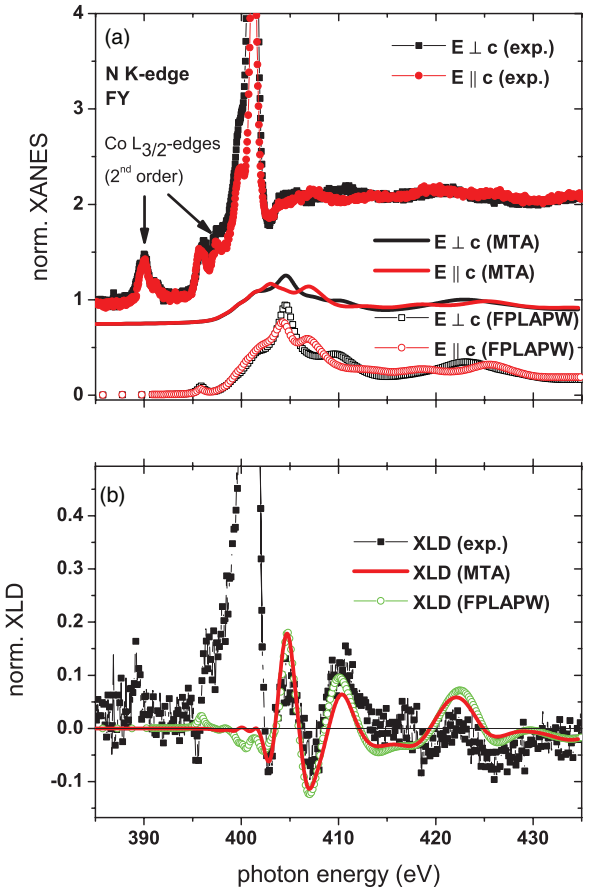


FIG. 5. (Color online) (a) Experimental XANES at the N $K$-edge for the film grown with $Ar:O_2:N_2 = 10 : 0.5 : 1$ (solid symbols) and simulated spectra of substitutional incorporation of N on O lattice sites ($N_O$). Simulations were performed with MTA (lines) and FPLAPW (open symbols). (b) Respective XLD spectra.

However, both XANES and XLD are still indicative of a predominant fraction of $N_2$ split interstitials which we tentatively ascribe to the lower cracking efficiency for $N_2$ during the reactive magnetron sputtering process compared to $O_2$. Since the formation of $N_2$ split interstitials is not supportive of $p$-type doping of ZnO, the resulting electric and magnetic properties of these Co:ZnO:N samples are beyond the scope of this work, which focuses on the actual incorporation of the N into the ZnO host lattice, and will be discussed elsewhere. It should be briefly noted that all samples, no matter if they are N doped or not, are found to be highly resistive, with the resistivity typically increasing with N doping (sheet resistance up to ∼200 GΩ). In addition, the temperature dependence of the resistivity typically indicates hopping-type conductivity,[30] presumably due to the columnar growth found for Co:ZnO (Ref. 18), which complicates the ability to draw reliable conclusions from Hall measurements.

## IV. CONCLUSION

In conclusion, we have used XANES to prove that nitrogen is incorporated within the ZnO lattice structure predominantly in its molecular form as $N_2$ split interstitials. The associated XLD is consistent with a preferential orientation of the $N_2$

molecules of 35° with respect to the *c* axis as predicted by DFT.[14] Only at very low $O_2$ and very high $N_2$ partial pressures is a small fraction of the nitrogen incorporated in its atomic form on substitutional O sites ($N_O$). Since only the latter N dopant configuration holds some promise towards *p*-type doping of ZnO, alternative strategies have to be found to increase the fraction of $N_O$ over the formation of $N_2$ split interstitials. On the other hand, the coexistence of $N_2$ split interstitials and $N_O$ enables the proper identification of the individual features of both dopant species in XANES and in XLD, which can serve as future reference for spectroscopic investigations to optimize the N incorporation in ZnO samples. Especially the XLD signatures at the N *K*-edge in comparison to the O *K*-edge are of great value in properly identifying the actual dopant species in a given specimen.

## ACKNOWLEDGMENTS

A.N. thanks the Deutsche Forschungsgemeinschaft (DFG) for financial support through the Heisenberg Programm. A.V. and A.G. thank the Russian Ministry of Education for providing the financial support and the UGINFO Computer Center of Southern Federal University for providing the computing time.

*daniel.schauries@uni-due.de

[1] A. Janotti and C. G. Van de Walle, Rep. Prog. Phys. **72**, 126501 (2009).
[2] T. Dietl, H. Ohno, F. Matsukura, J. Cibert, and D. Ferrand, Science **287**, 1019 (2000).
[3] N. A. Spalidin, Phys. Rev. B **69**, 125201 (2004).
[4] P. Fons, H. Tampo, A. V. Kolobov, M. Ohkubo, S. Niki, J. Tominaga, R. Carboni, F. Boscherini, and S. Friedrich, Phys. Rev. Lett. **96**, 045504 (2006).
[5] A. Kobayashi, O. F. Sankey, and J. D. Dow, Phys. Rev. B **28**, 946 (1983).
[6] J. L. Lyons, A. Janotti, and C. G. Van de Walle, Appl. Phys. Lett. **95**, 252105 (2009).
[7] M. C. Tarun, M. Z. Iqbal, and M. D. McCluskey, AIP Adv. **1**, 022105 (2011).
[8] X. M. Duan, C. Stampfl, M. M. M. Bilek, D. R. McKenzie, and S.-H. Wei, Phys. Rev. B **83**, 085202 (2011).
[9] C. H. Patterson, Phys. Rev. B **74**, 144432 (2006).
[10] D. C. Look and B. Claflin, Phys. Stat. Solidi B **241**, 624 (2004).
[11] A. Tsukazaki, M. Kubota, A. Othomo, T. Onuma, K. Ohtani, H. Ohno, S. F. Chichibu, and M. Kawasaki, Jpn. J. Appl. Phys. **44**, 643 (2005).
[12] C. W. Zou, X. D. Yan, J. Han, R. Q. Chen, W. Gao, and J. Metson, Appl. Phys. Lett. **94**, 171903 (2009).
[13] Y. Cui and F. Bruneval, Appl. Phys. Lett. **97**, 042108 (2010).
[14] E.-C. Lee, Y.-S. Kim, Y.-G. Jin, and K. J. Chang, Physica B: Conden. Matter **308–310**, 912 (2001); Phys. Rev. B **64**, 085120 (2001).
[15] J. B. Metson, H. J. Trodahl, B. J. Ruck, U. D. Lanke, and A. Bittar, Surf. Interface Anal. **35**, 719 (2003).
[16] Y. Chunga, J. C. Lee, and H. J. Shin, Appl. Phys. Lett. **86**, 022901 (2005).
[17] A. Ney, K. Ollefs, S. Ye, T. Kammermeier, V. Ney, T. C. Kaspar, S. A. Chambers, F. Wilhelm, and A. Rogalev, Phys. Rev. Lett. **100**, 157201 (2008).
[18] A. Ney, A. Kovács, V. Ney, S. Ye, K. Ollefs, T. Kammermeier, F. Wilhelm, A. Rogalev, and R. E. Dunin-Borkowski, New J. Phys. **13**, 103001 (2011).
[19] http://www.esrf.eu/UsersAndScience/Experiments/ElectStructMagn/ID08.
[20] A. Rogalev, J. Goulon, C. Goulon-Ginet, and C. Malgrange, Lect. Notes Phys. **565**, 61 (2001).
[21] J. P. Perdew, K. Burke, and M. Ernzerhof, Phys. Rev. Lett. **77**, 3865 (1996).
[22] G. Kresse and J. Furthmüller, Comput. Mater. Sci. **6**, 15 (1996); Phys. Rev. B **54**, 11169 (1996).
[23] J. P. Perdew, in *Electronic Structure of Solids '91*, edited by P. Ziesche and H. Eschrig (Akademie, Berlin, 1991).
[24] Y. Joly, Phys. Rev. B **63**, 125120 (2001).
[25] P. Blaha, K. Schwarz, G. K. H. Madsen, D. Kvasnicka, and J. Luitz, Computer code WIEN2K, Technische Universität Wien, Austria, 2001; P. Blaha, K. Schwarz, P. Sorantin, and S. B. Trickey, Comput. Phys. Commun. **59**, 399 (1990).
[26] E. H. Kisi and M. M. Elcombe, Acta Crystallogr., Sect. C: Cryst. Struct. Commun. **45**, 1867 (1989).
[27] M. O. Krause and J. H. Oliver, J. Phys. Chem. Ref. Data **8**, 329 (1979).
[28] A. P. Hitchcock and C. E. Brion, J. Electron Spectrosc. Relat. Phenom. **18**, 1 (1980).
[29] F. Sette, J. Stöhr, and A. P. Hitchcock, J. Chem. Phys. **81**, 4906 (1984).
[30] S. Ye, V. Ney, T. Kammermeier, K. Ollefs, S. Zhou, H. Schmidt, F. Wilhelm, A. Rogalev, and A. Ney, Phys. Rev. B **80**, 245321 (2009); S. Ye, V. Ney, T. Kammermeier, K. Ollefs, S. Zhou, H. Schmidt, and A. Ney, J. Phys.: Conf. Ser. **200**, 052034 (2010).